

BRD4 PROTAC Degradation Agent GNE-987 Inhibits Acute Myeloid Leukemia by Targeting Super Enhancers

Xu Sang

Department of Hematology, Children's Hospital of Soochow University

Yongping Zhang

Department of Hematology, Children's Hospital of Soochow University

Fang Fang

Institute of Pediatric Research, Children's Hospital of Soochow University

Li Gao

Department of Hematology, Children's Hospital of Soochow University

Yanfang Tao

Institute of Pediatric Research, Children's Hospital of Soochow University

Xiaolu Li

Institute of Pediatric Research, Children's Hospital of Soochow University

Zimu Zhang

Institute of Pediatric Research, Children's Hospital of Soochow University

Jianwei Wang

Institute of Pediatric Research, Children's Hospital of Soochow University

Yuanyuan Tian

Department of Hematology, Children's Hospital of Soochow University

Zhiheng Li

Institute of Pediatric Research, Children's Hospital of Soochow University

Di Yao

Department of Hematology, Children's Hospital of Soochow University

Yumeng Wu

Department of Hematology, Children's Hospital of Soochow University

Xinran Chu

Department of Hematology, Children's Hospital of Soochow University

Kunlong Zhang

Department of Hematology, Children's Hospital of Soochow University

Li Ma

Department of Hematology, Children's Hospital of Soochow University

Lihui Lu

Department of Hematology, Children's Hospital of Soochow University

Yanling Chen

Institute of Pediatric Research, Children's Hospital of Soochow University

Juanjuan Yu

Institute of Pediatric Research, Children's Hospital of Soochow University

Ran Zhuo

Institute of Pediatric Research, Children's Hospital of Soochow University

Shuiyan Wu

Department of Hematology, Children's Hospital of Soochow University

Zhen Zhang

Department of Pediatrics, The First Affiliated Hospital of Bengbu Medical College

Jian Pan (✉ panjian2019@suda.edu.cn)

Institute of Pediatric Research, Children's Hospital of Soochow University

Shaoyan Hu

Department of Hematology, Children's Hospital of Soochow University

Research Article

Keywords: BRD4, GNE-987, Acute myeloid leukemia, Super enhancers, LYL1

Posted Date: December 29th, 2021

DOI: <https://doi.org/10.21203/rs.3.rs-1204848/v1>

License: © ⓘ This work is licensed under a Creative Commons Attribution 4.0 International License.

[Read Full License](#)

Abstract

Background: Acute myeloid leukemia (AML) is a common hematological malignancy in children, with poor treatment effect and poor prognosis. Recent studies have shown that bromodomain and terminal protein inhibitors are promising antitumor drugs. As a new type of BRD4 PROTAC degradation agent, GNE-987 can slow down the growth rate of a variety of tumors and cause apoptosis, which has broad clinical prospects. However, the role of GNE-987 in AML is unclear. This study aims to explore the therapeutic effect of GNE-987 in AML and its underlying mechanism.

Methods: By studying public databases, the prognostic significance of BRD4 and the correlation between AML were evaluated, and the relationship between BRD4 and the overall survival rate of AML patients was also analyzed. After adding GNE-987 to the AML cell line, cell proliferation slowed down, cycle disorder, and apoptosis increased. In the cells treated with GNE-987, western-blotting was used to detect BRD2, BRD3, BRD4 and PARP proteins. The effect of GNE-987 on AML cells was analyzed in vivo. RNA-seq and chromatin immunoprecipitation sequencing (ChIP-seq) confirmed the function and molecular pathway of GNE-987 in processing AML.

Results: Compared with healthy donors, the expression of BRD4 in children's AML samples was higher than that of healthy donors. The high expression of BRD4 indicates a poor prognosis. GNE-987 inhibits AML cell proliferation by inhibiting the cell cycle and inducing apoptosis. BRD2, BRD3 and BRD4 are consistent with the decreased expression of VHL in AML cells. Compared with JQ1 and ARV-825, GNE-987 has a lower IC50 in AML cells. In the AML xenograft model, GNE-987 significantly reduced the liver and spleen infiltration of leukemia cells, increased the survival time of mice, and caused BRD4, Ki67 dysregulation and caspase3 activation. According to the analysis of RNA-seq and ChIP-seq, GNE-987 can inhibit AML by targeting numerous super-enhancers.

Conclusions: GNE-987 has strong anti-tumor activity in AML cell lines and primary child AML samples. GNE-987 works by degrading the BET protein, thereby effectively inhibiting the expression of super enhancers and related oncogenes (such as LYL1). These results indicate that GNE-987 has very broad prospects for the treatment of AML.

Background

Acute myeloid leukemia (AML) is the most common hematological malignancy in adults and ranks second in childhood hematological malignancies [1, 2]. It is a serious threat to children's physical and mental health. The pathogenesis of acute myeloid leukemia is unknown, it is mostly believed to be related to abnormal epigenetic events caused by DNA or chromatin modification [3]. The epigenetic target screening using shRNA library and genome-wide CRISPR library proves that the bromodomain and extraterminal (BET) protein family member BRD4 is the most important member of the BET family of histone reading proteins, which is essential to maintain AML [4, 5].

The acetylated lysine residues in histone H4 can bind to BETP, which provides the assembly of multi-molecular super enhancer complexes [6, 7]. The helix loop helix (HLH) transcription factor (TF) family contains key regulators of lymphocyte development and maturation, such as Tal1/SCL/TCL5, etc. [8]. The other two basic HLH (bHLH) TFs, LYL1 and Tal2, are closely related to Tal1 in structure. Studies have shown that LYL1 is considered to be a super enhancer associated gene that causes AML [9, 10]. MYC is one of the key oncogenes that rely on transcription mediated by the hyper enhancer complex containing BETP [11, 12]. LYL1 and MYC lack pockets that can be directly targeted by small molecules, and it is difficult to directly target them. Therefore, a lot of energy has been focused on indirect targeting strategies.

Some of the previous bromodomain containing 4 (BRD4) inhibitors, such as JQ1 and I-BET, by disrupting the binding of BETP to acetylated histones, provide a way to target transcription by disrupting the "super enhancer" transcription complex MYC means [11, 12]. However, these drugs usually lack the ability to continuously inhibit transcription, leading to drug resistance. Proteolytic chimeras (PROTACs) are bifunctional molecules that promote protein target degradation rather than inhibit activity as a therapeutic strategy. These molecules contain a motif (peptide or small molecule) that binds a protein target connected by a chemical linker to a motif that binds to E3-ubiquitin ligase. This allows E3-ubiquitin protein ligase to recruit to the protein target, selectively become the target of ubiquitination, and promote its degradation through the cell's endogenous proteasome degradation mechanism. PROTAC activity requires the formation of a ternary complex similar to a three-body structure in the 1:1:1 subunit stoichiometry, which contains the target protein, PROTAC and E3-ubiquitinated ligase [6, 13]. Traditional inhibitor molecules require a 1:1 stoichiometry to inhibit a single protein target molecule, and PROTAC can play a substoichiometric role, using one PROTAC molecule to promote the degradation of multiple copies of the target protein, because PROTAC is after protein degradation released. This allows for lower dosing concentrations, a larger therapeutic window, and reduces the need to maintain high intracellular compound concentrations. The effective time of targeting degraded proteins is also shorter, and the weaker and lower affinity region can be used as the target site. Therefore, it can target the previously difficult-to-degrade protein [14].

As a new type of BRD4 PROTAC degradation agent, GNE-987 is a ternary complex formed between BRD4 bromodomains 1 and 2 (Brd4B1 and Brd4B2) and VonHippelLindau (VHL) E3-ubiquitin ligase. BRD4 is an effective drug target affected by various cancers, while VHL is usually recruited by PROTACs to degrade various targets in vitro and in vivo. GNE-987 has previously been proven to be a more effective in vitro degradation product of BRD4 than standard PROTACs MZ1 and ARV-825. The half-life measurement results of the ternary complex based on SPR show that the Brd4B1 ternary complex is more stable than the ternary complex containing BRD4B2 [15]. The binding of GNE-987 to the target can improve the stability and pharmacokinetics in vivo, and effectively increase the degradation of Brd4 and the killing of tumor cells by GNE-987 [15]. GNE-987 inhibits proliferation and induces cell apoptosis more effectively than traditional BRD4 inhibitors, and has a longer-lasting drug effect, possibly through the rapid and durable degradation of BRD4 and inhibition of downstream targets. But at present, there is still no research on GNE-987 in AML. Therefore, we studied the anti-tumor activity of GNE-987 on BRD4 in AML,

and confirmed that it down-regulates the expression of many super enhancers and related oncogenes, such as LYL1, to determine an effective strategy for the treatment of children with AML.

Materials And Methods

Samples

In order to determine the potential utility of targeting BRD4 in the treatment of AML, we analyzed the expression of BRD4 based on public RNA-seq data in AML samples. The standardized gene expression data was used to assess the prognostic significance of BRD4 and the correlation between the two, and the overall survival rate of BRD4 and AML patients was also analyzed.

Cell culture

The human leukemia cell lines (NB4, Kasumi-1, HL-60, MV4-11 and K562) and mouse leukemia cell line (P388-D1) were all from the Chinese Academy of Sciences Cell Bank, they were all verified by short tandem repeat analysis in 2019 and 2020. Cells were cultured in RPMI1640 medium containing 10% fetal bovine serum (Termo Fisher Scientific), and penicillin and streptomycin (Millipore, Billerica, MA, USA), 37°C, 5% CO₂, cultured in a humidified incubator, and routinely tested for mycoplasma.

Cell viability determination

GNE-987 is dissolved in 100% DMSO, the stock solution has a concentration of 10 mmol, and it is placed in a refrigerator at -80°C. AML cells were planted in a 96-well cell culture plate with a cell density of 2×10^4 in each well, and were treated with GNE-987 with different concentration gradients. The primary leukemia cells were separated from the bone marrow of children by Ficoll-Hypaque centrifugation, and then planted in a 96-well plate with a density of 1×10^5 cells in the culture medium. Cells treated with 0.05% dimethyl sulfoxide (DMSO) in complete medium without GNE-987 were used as controls. After 24 hours of drug treatment, according to the manufacturer's instructions, the cell viability was determined by the Cell Counting Kit-8 (CCK-8) assay (Dojindo Molecular Technologies, Tokyo, Japan). Each concentration is in triplicate, repeated in at least three independent experiments. Graph Prism software 8.3.0 (GraphPad Software Inc., San Diego, CA, USA) was used to calculate the half maximum inhibitory concentration (IC₅₀) of GNE-987.

Soft agar clone formation analysis

Prepare 1.2% and 0.7% agarose, autoclave and place in a 55°C water bath, prepare 2×RPMI1640 medium containing 20% FBS, 2× penicillin and streptomycin, and filter out with a 0.2 micron filter bacteria. Lower layer gel: 1.2% agarose gel was mixed with 2× medium 1:1, added to a 6-well plate, 1.5ml per well, and

solidified at room temperature. Cell count: AML cells treated with GNE-987 at different concentration gradients were washed with PBS, mixed and diluted with new medium and adjusted to 5×10^3 / ml with 100ul of cells suspension in each well. Upper glue: Mix 0.7% agarose gel with 2× medium 1:1, add 100ul cell suspension, after mixing wells, add 1.5ml to each well. Put it in a 37°C, CO₂ incubator, add culture medium every three days, and harvest the cells after about 3 weeks. Count and compare the number of cells treated with different concentrations of GNE-987, and finally analyze to calculate the rate of monoclonal formation.

Preparation and infection of lentivirus

Short hairpin RNA (shRNA) targeting VHL (GGAGCCTAGTCAAGCCTGAGACATCCGTTGATGTGCAATGCG) constructed in the pLKO.1 lentiviral vector. The CDS region of the VHL gene was searched in pubmed, synthesized and constructed into the PLVX-EF1a-puro vector. Short hairpin RNA (shRNA) targeting LYL1 (Table 1) were constructed in the pLKO.1-puro lentiviral vector (IGE BIOTECHNOLOGY LTD, Guangzhou, China). When preparing lentivirus, envelope plasmid and packaging plasmid were purchased from Addgene (pMD2.G: #12,259; psPAX2: #12,260; Cambridge, MA, USA). Co-transfect pMD2.G, psPAX2 and the transfer plasmid with polyethyleneimine into 293FT cells (linear MW 25,000 Da, 5mg/ml, pH 7.0) (cat. No. 23966-1; Polysciences, Warrington, PA, USA) according to the manufacturer's instructions. After 6h, completely replace the medium with fresh medium. Collect the virus supernatant 48h after transfection and filter it with a 0.22µm filter. Then, AML cells were infected with lentivirus for 24 hours in the presence of 10 µg/mL polyene (Sigma-Aldrich). Screen stable cell lines with puromycin (Sigma-Aldrich).

RNA preparation and real-time PCR expression analysis

Total RNA was extracted from cell pellets using TRIzol® reagent (Invitrogen, CA, USA), according to the manufacturer's protocol. For cDNA synthesis, 1µg of total RNA was converted to cDNA using a High-Capacity cDNA Reverse Transcription Kit (Applied Biosystems, CA, USA). Quantitative real-time PCR analysis was carried out using LightCycler® 480 SYBR Green I Master mix (cat. No. 04707516001; Roche, Penzberg, Germany) with a LightCycler 480 Real Time System (Roche), according to the manufacturer's protocol. mRNA expression levels were calculated using the Ct method with glyceraldehyde 3-phosphate dehydrogenase (GAPDH) expression as an internal reference. Primer sequences are listed in Table 2.

Cellcycleanalysis

24 hours after adding different concentrations of GNE-987 to the AML cell line, the cell line was trypsinized, washed and fixed in 70% ethanol at 4°C overnight. Then wash the cells with cold phosphate buffered saline (PBS) and resuspend them in 0.5 ml of PI/RNase staining fermentation broth (cat. No. 550825; BD Pharmingen™, San Diego, CA, USA), then incubate at room temperature for 15 min. Flow

cytometry was performed using Beckman Gallios™ Flow Cytometer (Beckman, Krefeld, Germany), and the cell cycle was analyzed using MultiCycle AV DNA analysis software (Verity Software House, Topsham, ME, USA).

Cell apoptosis analysis

Add different concentrations of GNE-987 to the cell line, collect it after 24h, centrifuge at 2000rpm, 3min, discard the supernatant, wash once with cold PBS, centrifuge at 4000rpm, 3min, take the supernatant, suspend it in 1× binding buffer, use fluorescein isothiocyanate (FITC)- AnnexinV apoptosis kit and PI solution staining (cat. No. 556420; BD Biosciences, Franklin Lakes, NJ, USA), follow the manufacturer's instructions. Cell counting method was used to analyze cell apoptosis (Beckman Gallios™ Flow Cytometer; Beckman).

Western blotting analysis

Use the following antibodies for Western blotting analysis, BRD2 (cat.No.5848 s; 1:1000; Cell Signaling Technology, Boston, MA, USA), BRD3 (cat. No. 11859-1-AP; 1:1000; Proteintech, Chicago, IL, USA), BRD4 (cat. No. 13440 s; 1:1000; Cell Signaling Technology), VHL (cat. No. 68547 s; 1:1000; Cell Signaling Technology), LYL1 (cat. No. sc-374164; 1:1000; Santa Cruz Biotechnology), and PARP (cat. No. 9542; 1:1000; Cell Signaling Technology) with glyceraldehyde 3-phosphate dehydrogenase (GAPDH) (cat. No. MA3374; 1:1000; Millipore) as a reference protein. Peroxidase-conjugated Affinire goat anti-rabbit IgG(H+L) IgG(H+L) (cat. 111-035-003; 1:5000) and goat anti-mouse IgG(H+L) (cat. No. 115-035-003; 1:5000) purchased from Jackson ImmunoResearch Laboratories, Inc. (West Grove, PA, USA). Define the role of the proteasome, MG132 (cat. No. 474787, Sigma-Aldrich, St. Louis, MO, USA) inhibits the proteasome activity. After 24h treatment with different concentrations of GNE-987, the cells were collected, and the BRD2, BRD3, BRD4, PARP, VHL, LYL1 and GAPDH proteins were determined by Western blotting analysis.

Study the anti-tumor effect of GNE-987 in Vivo

All experimental animal procedures in this study were approved and licensed by the Animal Care and Use Committee of Children's Hospital of Soochow University (CAMSU-AP#: JP-2018-1). SPF grade BALB/c mice were from Linghang Biotechnology Co., Ltd. (Shanghai, China). Five-week-old female mice (n=5 in each group) were injected with 3×10^5 P388-D1 cells via the tail vein. 2 days after injection of cells, each mouse was injected with luciferase into the abdominal cavity and immediately anesthetized with isoflurane gas. Then, each group of mice was imaged using the NightOWL in-vivo Imaging System (BERTHOLD, Germany). After the tumor fluorescence signal appeared (Day 2), mice in the experimental group were injected intraperitoneally with 0.5mg/KgGNE-987; in the control group, mice were injected intraperitoneally with GNE-987 (5%®HS15), once a day, 9 times in total (Day2~Day10). Continue to use

the NightOWL in-vivo Imaging System to image each group of mice on the 4th, 7th, and 10th days. The mice were weighed daily to observe the color and mobility of the fur. The liver, spleen, kidneys and intestines of the experimental group and control group mice were collected, and the organ size was observed and weighed. Each organ specimen was subjected to immunohistochemistry and HE staining. Primary antibody BRD4 (cat: No. 13440 s; 1:1000; Cell Signaling Technology), cleaved-caspase 3 (cat: No. GB11009-1, 1:300, Servicebio, Boston, MA, USA) and Ki67 (cat: No. ab15580, 1:300, Abcam, Cambridge, UK), has been used according to the manufacturer's recommendations.

RNA sequencing and data processing

RNA-seq was carried out according to the protocols suggested by Novogene Bioinformatics Technology Co., Ltd. (Beijing, China). First, the total RNA was reverse transcribed into cDNA to construct a library, and then the cDNA library was sequenced. Filter the original reads and map the clean reads according to HISAT. Then calculate the gene expression level (as the fragment mapped per million reads per kilobase exon model). Using DESeq2 analysis, differentially expressed genes were identified ($P < 0.05$ and fold change > 2 or fold change < 0.5). For enrichment analysis, differentially expressed genes were analyzed using the GSEA software (UC San Diego and Broad Institute,).

Chromatin immunoprecipitation sequencing (ChIP-seq)

$3-5 \times 10^7$ cells were cross-linked with 1% formaldehyde for 10 minutes, and neutralized with 1.25M glycine at room temperature for 5 minutes. Use Bioruptor (Diagenode, Liège, Belgium) to collect, lyse and sonicate fixed cells. Sonicated chromatin was incubated with anti-histone H3 (acetyl K27) antibody (cat. No. ab4729; Abcam, Cambridge, UK) overnight at 4°C. DNA was eluted and purified using a QIAquick PCR purification kit (cat. No. 208106; Qiagen, Hilden, Germany). The samples are sequenced on the novaseq 6000 platform (Novogene Bioinformatics Technology Co., Ltd. Beijing, China) and a BGISEQ 2000 platform (Beijing Genomics Institute (Shenzhen, China)). Raw data of ChIP-Seq H3K27ac analysis was aligned to the reference genome (UCSC hg38) using Bowtie2 (v 2.3.5) [17], with alignment parameters -p 4 -q -x. Peaks were identified using MACS2 (v2.0.9) [18], with parameters -g hs -n test -B -q 0.01. The bedgraph files generated by MACS2 were converted to bigwig files using the UCSC bedGraphToBigWig tool, and then bigwig files were visualized by Integrative Genomics Viewer (IGV) [19]. Super-enhancers were then identified using the ROSE (Rank Order of Super Enhancers) method [20, 21], with parameters -s 12500 -t 2000.

Statistical analysis

All experiments were carried out independently at least three times. Statistical analysis was carried out using SPSS software version 21.0 (IBM Corporation, NY, USA). Survival analysis was performed by Kaplan-Meier estimates with log-rank tests. Student's t test was used to compare the percentage of

apoptosis, BRD4 mRNA level and cell viability. Normally distributed measurement data are expressed as mean± standard deviation. Use the t test to compare the differences between the two groups. Non-normally distributed data are expressed in quartiles (usually the median plus the range) and are compared using the Mann-Whitney U test. All experiments are two-tailed, P<0.05 is statistically significant.

Results

BRD4 is over expressed in AML patients and is associated with poor prognosis

Compared with the normal population, BRD4 expression in AML patients increased significantly according to the GEPIA database (<http://gepia.cancer-pku.cn/index.html>, Fig. 1a). The expected overall survival rate of high BRD4 expression in AML patients is lower than that of low expression patients according to the R2 database (<https://hgserver1.amc.nl/cgi-bin/r2/main.cgi>, Fig. 1b) and the GEPIA database (<http://gepia.cancer-pku.cn/index.html>, Fig. 1c). These results suggest that BRD4 will become a potential therapeutic target for pediatric AML.

GNE-987 causes the death of the AML cell lines and inhibits its growth

The cell viability curve after adding different concentration gradients of GNE-987 to AML cells is shown in the Fig. 2a. The IC50 and 95% CI of GNE-987 in different AML cells is shown in Fig. 2b. It can be seen that the half-inhibitory concentration value is low, at the nmol level. The BET family members are universally expressed in myeloid leukemia cell lines (Fig. 2c). Fluorescence microscopy showed that the vast majority of AML cells died 24 hours after the addition of GNE-987 (Fig. 2d). After adding GNE-987 to AML cells, compared with the group without GNE-987, the cell growth was slower and the number of clones decreased, and the difference was statistically significant (Fig. 2e, f).

GNE-987 blocked cell cycle and promoted apoptosis of AML cell lines

By influencing the cell cycle and promoting cell apoptosis, GNE-987 has higher cytotoxicity in AML. We detected cell cycle defects by PI staining. Most AML cells were distributed in the G1/S phase, but after 24 hours of treatment with GNE-987, the proportion of cells in the G1 phase increased significantly (Fig. 3a). In addition, GNE-987 continued to treat the cells for 24 hours, which increased the apoptotic rate of the AML cell lines (Fig. 3b).

GENE-987 causes degradation of BET protein in AML cell lines

GENE-987 is designed with PROTAC technology to selectively degrade target proteins through the ubiquitin proteasome system. Therefore, we analyzed the BET protein expression of AML cell lines after treatment with 5 different concentrations of GNE-987 for 24 hours. Western blotting analysis showed that GNE-987 induced degradation of BET protein and increased PARP (Fig. 4a). BRD4 protein was almost completely degraded in the AML cell lines treated with GNE-987. In addition to BRD4, GNE-987 also reduced the expression levels of BRD2 and BRD3 proteins. These data indicate that GNE-987 down-regulates BET protein expression in AML cells. We also compared the drug sensitivity test of GNE-987, JQ1 and ARV-825 gradient treatment of AML cell lines for 24 hours (Fig. 4b). It can be seen that the effect of GNE-987 is much higher than that of JQ1 and ARV-825. We added JQ1 and ARV-825 to NB4 cells 24 hours later to observe the degradation efficiency of BET protein. As shown in Fig. 4c, after adding JQ1 and ARV-825 at the highest concentration of 100nM, the BET protein is almost not degraded.

VHL is the key E3 enzyme for the function of GNE-987 and the degradation of BRDs protein depends on the proteasome

VHL is a powerful assistant of GNE-987. We tested the expression of VHL in AML cell lines. VHL is widely expressed in myeloid leukemia cell lines (Fig. 5a). The molecular structure of GNE-987 contains BRD4 ligand and VHL ligand (Fig. 5b). After adding different concentrations of GNE-987 to NB4, Kasumi-1, HL-60 and MV4-11 cell lines, the expression of VHL was also significantly reduced when BET was consumed (Fig. 5c). In addition, we successfully transfected VHL knockdown and VHL over-expression vectors into NB4 and Kasumi-1 cells, and verified their expression by Western blotting analysis (Fig. 5d). GNE-987 has the ability to recruit VHL. To illustrate this hypothesis, we did the following experiment. Down-regulation of VHL increased the half-inhibitory concentration of GNE-987 in NB4 and Kasumi-1 cells; while over-expression of VHL decreased the half-inhibitory concentration of GNE-987 in these cells. This shows that VHL is the key E3 enzyme for the function of GNE987 (Fig. 5e). In order to determine the role of the proteasome in the degradation of BRDs induced by GNE-987, we used the proteasome inhibitor MG132 to evaluate the activity of the proteasome (Fig. 5f). MG132 is widely used to inhibit the proteasome activity. The results showed that by blocking the proteasome with MG132, BRDs protein increased in a dose-dependent manner. In summary, these data indicate that GNE-987 induces growth inhibition through a VHL-mediated mechanism.

GENE-987 has a strong anti-tumor effect on patients with primary AML

We used two diagnostic AML samples from children to determine whether the primary pediatric AML cells are sensitive to GNE-987 treatment. The clinical and molecular characteristics of 2 cases of primary AML in children are shown in the Fig. 6a. Consistent with the results of the previous AML cell lines, the sensitivity of primary cells to GNE-987 is much higher than that of JQ1 and ARV-825 (Fig. 6b). We treated primary cells with DMSO or different doses of GNE-987 and found that GNE-987 promoted cell apoptosis (Fig. 6c). In GNE-987-treated primary AML cells, the expression levels of BRD2, BRD3, BRD4 and VHL proteins also decreased, and PARP increased, which was consistent with the results of the cell line. In GNE-987-treated cultures, LYL1 protein levels were also significantly reduced (Fig. 6d).

In vivo studies confirm that GNE-987 has a powerful anti-tumor effect

In order to further study the in vivo activity of GNE-987, we used P388-D1 cells to establish a preclinical model of AML. The entire operation process is shown in the Fig. 7a. On days 2, 4, 7 and 10, we used the NightOWL in vivo imaging system to image each group of mice (Fig. 7b). Compared with the control group, the liver and spleen infiltration of the mice in the GNE-987 treatment group was significantly reduced. The histogram of tumor luminous flux showed that GNE-987 group was much lower than the control group (Fig. 7c). By comparing the survival time of the two groups of mice, it is proved that GNE-987 can prolong the lifespan of mice (Fig. 7d). Comparing the body weight of the two groups of mice, the difference was not statistically significant, indicating that GNE-987 has no obvious side effects (Fig. 7e). The mice were dissected to obtain liver and spleen specimens. It can be seen that the size and weight of the liver and spleen of the mice treated with GNE-987 were significantly smaller than those of the control group (Fig. 7f, g). In the spleen of GNE-987-treated mice, BRD4 and Ki67-positive cells decreased, while the proportion of cleaved-caspase 3-positive cells in the spleen of GNE-987-treated mice increased (Fig. 7h). The HE stained sections of the liver, spleen, kidney, and intestine of the two groups of mice showed that the tumor cells of the liver and spleen were significantly reduced after GNE-987 treatment, the pathological changes of the kidney were not obvious, and the intestinal injury was mild, which also indicated that GNE-987 did less damage to the organs (Fig. 7i).

GNE987 treatment down-regulated the expression of super enhancer related gene LYL1 in AML cells

We performed RNA-seq gene expression profile analysis on NB4 cells after GNE987 treatment. Compared with the DMSO-treated control group, in GNE987-treated NB4 cells, the expression of 7553 genes was up-regulated and the expression of 4281 genes was down-regulated (Fig. 8a). The GSEA diagram shows that the differently expressed genes are enriched in apoptosis, KRAS and P53 signaling pathway (Fig. 8c). Next, we combined ChIP-seq super enhancer profiling and gene expression analysis to determine the key oncogenes involved in the pathogenesis of AML. We performed H3K27ac ChIP-Seq detection in NB4 cells, and filtered 215 super-enhancer-related genes in NB4 cells which were also down-regulated in GNE987-

treated NB4 cells (Fig. 8b). LYL1 is involved in the 215 genes. In fact, after AML cell lines were treated with GNE987, the expression of super enhancer-related gene LYL1 was also significantly down-regulated (Fig. 9a). Detection of LYL1 knockdown efficiency in NB4 cell line and Kasumi-1 cell line by qPCR and western blotting (Fig. 9b, c). Consistent with the expected results, after we down-regulated LYL1, we observed significant apoptosis induction in NB4 and Kasumi-1 cell lines. Among them, the apoptosis caused by sh-LYL1-3 was the most obvious, and the difference was statistically significant (Fig. 9d, e). In addition, gene knockout analysis showed that down-regulation of LYL1 significantly inhibited the growth of NB4 and Kasumi-1 cell lines (Fig. 9f).

Discussion

AML is a relatively common malignant tumor in children. It has the characteristics of strong invasiveness, poor prognosis, and complex etiology [22]. It is necessary to understand its pathogenesis in detail to improve the treatment and prognosis of AML [23]. BRD4 plays an important role in a variety of cancer types, including prostate cancer, lung cancer, melanoma, and hematological malignancies [24-26]. However, the biological significance of BRD4 in AML is unclear. We initially detected the expression of BRD4 and found that in CCLE samples, BRD4 is the top gene in AML cell lines compared to other types of cancer cell lines. The RNA-seq analysis in this study showed that the BRD4mRNA expression level of AML samples was higher than that of healthy samples; survival analysis showed that BRD4 led to a worse prognosis in children with AML. Studies have shown that BRD4 can accumulate in super enhancer regions involved in the control of key oncogenes, such as c-Myc, Bcl-xl and Bcl-2, etc [15, 24-26]. This suggests that it can be used as a new therapeutic target to improve the prognosis of AML patients.

There are many BRD4 inhibitors, such as JQ1 and OTX015, which have obvious drawbacks. For example, these drugs can only inhibit the growth of a small number of tumor cells in patients with stage I, promote cell apoptosis, and lack the ability to continuously inhibit transcription [1, 15]. Therefore, new ideas for improving BRD4 inhibition are urgently needed, and GNE-987 came into being. GNE-987 is designed to be an irreversible covalent inhibitor that can achieve the desired effect at a lower drug concentration. The ternary complexes of BRD4B1 or BRD4B2 and VHL promoted by Protac GNE-987 were determined by high-resolution natural mass spectrometry. Moreover, the ternary complex of BRD4B1 forms larger than the ternary complex containing BRD4B2, which indicates that the complex containing BRD4B1 is more stable [27]. Through the direct measurement of natural mass spectrometry, we understand the relationship between the ligase and the target in PROTAC, the number of ternary complexes formed, and the balance between the binary and ternary interactions that drive the "hook effect" [28].

As a new type of BRD4 degradation agent, our research found that the IC50 of GNE-987 in AML cell lines is less than 100nmol, which is significantly lower than that of JQ1 and ARV-825. Our research results show that GNE-987 can significantly reduce the growth of AML cells in vivo and in vitro by slowing down cell proliferation, interfering with the cell cycle, and accelerating cell apoptosis. These results are consistent with the observations of BRD4 inhibitors such as JQ1 and ARV-825 on solid tumors and AML [29-31], and GNE-987 has more advantages than JQ1 and ARV-825 [32, 33]. BET proteins, including

BRD2, BRD3, BRD4, etc., are epigenome readers known to be associated with acetylated chromatin and transcriptional regulation. Our research found that after treatment with GNE-987, not only BRD4 can be degraded, but the levels of BRD2 and BRD3 proteins are reduced, which is similar to the results of other BET inhibitors[15]. Due to the high homology between BET family members, GNE-987 can bind to all BET family members. GNE-987 is a PROTAC targeting BRD4 and BET family proteins. It can undergo VHL-mediated proteasome degradation and can greatly consume BET protein. This can describe the discovery of a new and highly active chimeric BET degradation agent, which contains an effective BET binder/inhibitor, a VHL binding fragment, and a 10 methylene spacer. VHL targets the chimeric BET degrading agent payload to deliver to the tumor, which may explain the potent killing effect of GNE-987 on AML.

At present, super-enhancers are a hot spot in tumor research. Compared with ordinary enhancers, super-enhancers have the ability to recruit a large number of transcription/cofactors and induce the transcription of many target genes. Studies have shown that super enhancers are closely related to oncogenes [34]. But so far, the biological significance of super-enhancers in AML is not clear, so it is urgent to study the key super-enhancers in AML. In this study, we found that adding GNE-987 to AML cells can down-regulate the expression of super-enhancer-related genes, including LYL1. Previous studies have shown that LYL1 can play a role in renal clear cell carcinoma and osteosarcoma, and copy number amplification occurs in glioma [35-37]. Studies have shown that the expression of LYL1 in AML is higher than that of normal bone marrow [9]. LYL1 plays a role in the seven transcription factors of human CD34+ hematopoietic stem progenitor cells (hsps), and LYL1 can also affect the prognosis of AML [38]. In general, in our study, while GNE-987 consumed BET in AML cell lines, it also down-regulated the expression of multiple super-enhancer-related genes, including LYL1. These findings provide new insights into the pathophysiology of AML and provide a new direction for the treatment of AML.

Conclusion

In summary, the results of this study show that GNE-987 has strong anti-tumor activity in AML cell lines, primary child AML samples and in vivo experiments. GNE-987 plays its anti-tumor effect by degrading BET protein, and VHL is the key E3 enzyme for GNE-987 to play a role. Not only that, GNE-987 can also down-regulate the expression of super-enhancer-related genes in AML cells, including the expression of LYL1, which is closely related to AML. These results indicate that GNE-987 may be a promising treatment for AML and is worthy of further study.

Abbreviations

AML: Acute myeloid leukemia; BET: Bromodomain and extra terminal; BRD4: Bromodomain-containing protein 4; CCK-8: Cell Counting Kit-8; IC50: Half-maximal inhibitory concentration; PBS: Phosphate-buffered saline; PCR: Polymerase chain reaction; shRNA: Short hairpin RNA.

Declarations

Ethics approval and consent to participate

This study was provided by the Children's Hospital of Soochow University Ethics Committee, Suzhou, China (No. SUEC2000-021 & No. SUEC2011-037). The Animal Care Committee of Suzhou College 1 approved all animal studies 2, Suzhou, China (approval number: CAM-SU-AP#: JP-2018-1). Written informed consent was obtained from each participating individual's guardian.

Consent for publication

Not applicable.

Availability of data and materials

The data used and / or analyzed during the current study are available from the corresponding author on reasonable request (GSE188750, GSE188891).

Competing interests

The author declares that there is no conflict of interest.

Funding

This research was supported by grants from the National Natural Science Foundation (81770145, 81802499, 81971867, 81970163, 81902534, 82072767, 52003183, 82141110); Natural Science Foundation of Jiangsu Province (SBK2019021442, BK20190185, BK20190186, BK20191175); the Universities Natural Science Foundation of Jiangsu Province (No. 16KJB310014); Jiangsu province's science and technology support program (Social Development) project (BE2021657, BE2021654); Jiangsu Province Key R&D Program (Social Development) Projects (BE2020659); Department of Pediatrics Clinical Center of Suzhou (Szzx201504); Gusu Health Talents program of Soochow city (2020-104); the Applied Foundational Research of Medical and Health Care of Suzhou City (SYS2019080, SYS2019082, SYS2019077, SYS2020150, SYS2020151, GSWS2020039); the Science and Technology Development Project of Suzhou City (SKJY2021111, SKJY2021112); the Science and Technology Project of Soochow (SS2019011).

Author contributions

JP and SYH designed and directed the study; XS, YPZ, FF and LG performed most of the experiments, analyzed the data, and wrote the paper; YFT, XLL, ZMZ, JWW and YYT helped with statistical analysis; ZHL, DY, YMW and XRC performed part of the experiments; XLL, ZMZ and JWW performed lentivirus preparation and transfection; KLZ, LM and LHL participated in western blotting, PCR, and in vitro experiments; YLC and JJY collected clinical data; RZ SW and ZZ supported the design of primers for real-time PCR; YPZ and YMW helped with the apoptosis and cell cycle analysis; XLL, ZMZ and JWW participated in plasmid construction. All authors read and approved the final manuscript.

Acknowledgments

We would like to thank the department of Hematology, Children's Hospital of Soochow University, for the support in this study.

Authors' information

¹ Department of Hematology, Children's Hospital of Soochow University, No. 92 Zhongnan Street, SIP, Suzhou 215003, Jiangsu, China.

² Department of Pediatrics, The First Affiliated Hospital of Bengbu Medical College, No. 287 Changhuai Road, Bengbu 233004, Anhui, China.

³ Institute of Pediatric Research, Children's Hospital of Soochow University, No. 92 Zhongnan Street, SIP, Suzhou 215003, Jiangsu, China.

References

1. M. Loosveld, R. Castellano, S. Gon, A. Goubard, T. Crouzet, L. Pouyet, T. Prebet, N. Vey, B. Nadel, Y. Collette, D. Payet-Bornet, Therapeutic targeting of c-Myc in T-cell acute lymphoblastic leukemia, T-ALL. *Oncotarget* (2014) 5: 3168-72 DOI: 10.18632/oncotarget.1873.
2. I. De Kouchkovsky, M. Abdul-Hay, 'Acute myeloid leukemia: a comprehensive review and 2016 update'. *Blood Cancer J* (2016) 6: e441 DOI: 10.1038/bcj.2016.50.
3. J. Chen, O. Odenike, J.D. Rowley, Leukaemogenesis: more than mutant genes. *Nat Rev Cancer* (2010) 10: 23-36 DOI: 10.1038/nrc2765.
4. J. Zuber, J. Shi, E. Wang, A.R. Rappaport, H. Herrmann, E.A. Sison, D. Magoon, J. Qi, K. Blatt, M. Wunderlich, M.J. Taylor, C. Johns, A. Chicas, J.C. Mulloy, S.C. Kogan, P. Brown, P. Valent, J.E. Bradner,

- S.W. Lowe, C.R. Vakoc, RNAi screen identifies Brd4 as a therapeutic target in acute myeloid leukaemia. *Nature* (2011) 478: 524-8 DOI: 10.1038/nature10334.
5. K. Tzelepis, H. Koike-Yusa, E. De Braekeleer, Y. Li, E. Metzakopian, O.M. Dovey, A. Mupo, V. Grinkevich, M. Li, M. Mazan, M. Gozdecka, S. Ohnishi, J. Cooper, M. Patel, T. McKerrell, B. Chen, A.F. Domingues, P. Gallipoli, S. Teichmann, H. Ponstingl, U. McDermott, J. Saez-Rodriguez, B.J.P. Huntly, F. Iorio, C. Pina, G.S. Vassiliou, K. Yusa, A CRISPR Dropout Screen Identifies Genetic Vulnerabilities and Therapeutic Targets in Acute Myeloid Leukemia. *Cell Rep* (2016) 17: 1193-205 DOI: 10.1016/j.celrep.2016.09.079.
 6. P. Filippakopoulos, S. Knapp, Targeting bromodomains: epigenetic readers of lysine acetylation. *Nat Rev Drug Discov* (2014) 13: 337-56 DOI: 10.1038/nrd4286.
 7. I.A. Asangani, V.L. Dommeti, X. Wang, R. Malik, M. Cieslik, R. Yang, J. Escara-Wilke, K. Wilder-Romans, S. Dhanireddy, C. Engelke, M.K. Iyer, X. Jing, Y.M. Wu, X. Cao, Z.S. Qin, S. Wang, F.Y. Feng, A.M. Chinnaiyan, Therapeutic targeting of BET bromodomain proteins in castration-resistant prostate cancer. *Nature* (2014) 510: 278-82 DOI: 10.1038/nature13229.
 8. S. Greenbaum, Y. Zhuang, Regulation of early lymphocyte development by E2A family proteins. *Semin Immunol* (2002) 14: 405-14 DOI: 10.1016/s1044532302000751.
 9. Y.S. Meng, H. Khoury, J.E. Dick, M.D. Minden, Oncogenic potential of the transcription factor LYL1 in acute myeloblastic leukemia. *Leukemia* (2005) 19: 1941-7 DOI: 10.1038/sj.leu.2403836.
 10. Y. Natkunam, S. Zhao, D.Y. Mason, J. Chen, B. Taidi, M. Jones, A.S. Hammer, S. Hamilton Dutoit, I.S. Lossos, R. Levy, The oncoprotein LMO2 is expressed in normal germinal-center B cells and in human B-cell lymphomas. *Blood* (2007) 109: 1636-42 DOI: 10.1182/blood-2006-08-039024.
 11. P. Filippakopoulos, J. Qi, S. Picaud, Y. Shen, W.B. Smith, O. Fedorov, E.M. Morse, T. Keates, T.T. Hickman, I. Felletar, M. Philpott, S. Munro, M.R. McKeown, Y. Wang, A.L. Christie, N. West, M.J. Cameron, B. Schwartz, T.D. Heightman, N. La Thangue, C.A. French, O. Wiest, A.L. Kung, S. Knapp, J.E. Bradner, Selective inhibition of BET bromodomains. *Nature* (2010) 468: 1067-73 DOI: 10.1038/nature09504.
 12. J. Shi, W.A. Whyte, C.J. Zepeda-Mendoza, J.P. Milazzo, C. Shen, J.S. Roe, J.L. Minder, F. Mercan, E. Wang, M.A. Eckersley-Maslin, A.E. Campbell, S. Kawaoka, S. Shareef, Z. Zhu, J. Kendall, M. Muhar, C. Haslinger, M. Yu, R.G. Roeder, M.H. Wigler, G.A. Blobel, J. Zuber, D.L. Spector, R.A. Young, C.R. Vakoc, Role of SWI/SNF in acute leukemia maintenance and enhancer-mediated Myc regulation. *Genes Dev* (2013) 27: 2648-62 DOI: 10.1101/gad.232710.113.
 13. M.A. Dawson, R.K. Prinjha, A. Dittmann, G. Giotopoulos, M. Bantscheff, W.I. Chan, S.C. Robson, C.W. Chung, C. Hopf, M.M. Savitski, C. Huthmacher, E. Gudgin, D. Lugo, S. Beinke, T.D. Chapman, E.J. Roberts, P.E. Soden, K.R. Auger, O. Mirguet, K. Doehner, R. Delwel, A.K. Burnett, P. Jeffrey, G. Drewes, K. Lee, B.J. Huntly, T. Kouzarides, Inhibition of BET recruitment to chromatin as an effective treatment for MLL-fusion leukaemia. *Nature* (2011) 478: 529-33 DOI: 10.1038/nature10509.
 14. M. Jung, M. Philpott, S. Müller, J. Schulze, V. Badock, U. Eberspächer, D. Moosmayer, B. Bader, N. Schmees, A. Fernández-Montalván, B. Haendler, Affinity map of bromodomain protein 4 (BRD4)

- interactions with the histone H4 tail and the small molecule inhibitor JQ1. *J Biol Chem* (2014) 289: 9304-19 DOI: 10.1074/jbc.M113.523019.
15. D.T. Saenz, W. Fiskus, Y. Qian, T. Manshouri, K. Rajapakshe, K. Raina, K.G. Coleman, A.P. Crew, A. Shen, C.P. Mill, B. Sun, P. Qiu, T.M. Kadia, N. Pemmaraju, C. DiNardo, M.S. Kim, A.J. Nowak, C. Coarfa, C.M. Crews, S. Verstovsek, K.N. Bhalla, Novel BET protein proteolysis-targeting chimera exerts superior lethal activity than bromodomain inhibitor (BETi) against post-myeloproliferative neoplasm secondary (s) AML cells. *Leukemia* (2017) 31: 1951-61 DOI: 10.1038/leu.2016.393.
 16. G. Yu, L.G. Wang, Y. Han, Q.Y. He, clusterProfiler: an R package for comparing biological themes among gene clusters. *Omics* (2012) 16: 284-7 DOI: 10.1089/omi.2011.0118.
 17. B. Langmead, S.L. Salzberg, Fast gapped-read alignment with Bowtie 2. *Nat Methods* (2012) 9: 357-9 DOI: 10.1038/nmeth.1923.
 18. Y. Zhang, T. Liu, C.A. Meyer, J. Eeckhoute, D.S. Johnson, B.E. Bernstein, C. Nusbaum, R.M. Myers, M. Brown, W. Li, X.S. Liu, Model-based analysis of ChIP-Seq (MACS). *Genome Biol* (2008) 9: R137 DOI: 10.1186/gb-2008-9-9-r137.
 19. J.T. Robinson, H. Thorvaldsdóttir, W. Winckler, M. Guttman, E.S. Lander, G. Getz, J.P. Mesirov, Integrative genomics viewer. *Nat Biotechnol* (2011) 29: 24-6 DOI: 10.1038/nbt.1754.
 20. W.A. Whyte, D.A. Orlando, D. Hnisz, B.J. Abraham, C.Y. Lin, M.H. Kagey, P.B. Rahl, T.I. Lee, R.A. Young, Master transcription factors and mediator establish super-enhancers at key cell identity genes. *Cell* (2013) 153: 307-19 DOI: 10.1016/j.cell.2013.03.035.
 21. J. Lovén, H.A. Hoke, C.Y. Lin, A. Lau, D.A. Orlando, C.R. Vakoc, J.E. Bradner, T.I. Lee, R.A. Young, Selective inhibition of tumor oncogenes by disruption of super-enhancers. *Cell* (2013) 153: 320-34 DOI: 10.1016/j.cell.2013.03.036.
 22. K. Doucette, J. Karp, C. Lai, Advances in therapeutic options for newly diagnosed, high-risk AML patients. *Ther Adv Hematol* (2021) 12: 20406207211001138 DOI: 10.1177/20406207211001138.
 23. H. Kantarjian, Acute myeloid leukemia—major progress over four decades and glimpses into the future. *Am J Hematol* (2016) 91: 131-45 DOI: 10.1002/ajh.24246.
 24. Y.F. Liao, Y.B. Wu, X. Long, S.Q. Zhu, C. Jin, J.J. Xu, J.Y. Ding, High level of BRD4 promotes non-small cell lung cancer progression. *Oncotarget* (2016) 7: 9491-500 DOI: 10.18632/oncotarget.7068.
 25. P. Valent, J. Zuber, BRD4: a BET(ter) target for the treatment of AML? *Cell Cycle* (2014) 13: 689-90 DOI: 10.4161/cc.27859.
 26. J. Alsarraj, K.W. Hunter, Bromodomain-Containing Protein 4: A Dynamic Regulator of Breast Cancer Metastasis through Modulation of the Extracellular Matrix. *Int J Breast Cancer* (2012) 2012: 670632 DOI: 10.1155/2012/670632.
 27. M.M. Coudé, T. Braun, J. Berrou, M. Dupont, S. Bertrand, A. Masse, E. Raffoux, R. Itzykson, M. Delord, M.E. Riveiro, P. Herait, A. Baruchel, H. Dombret, C. Gardin, BET inhibitor OTX015 targets BRD2 and BRD4 and decreases c-MYC in acute leukemia cells. *Oncotarget* (2015) 6: 17698-712 DOI: 10.18632/oncotarget.4131.

28. R. Beveridge, D. Kessler, K. Rumpel, P. Ettmayer, A. Meinhart, T. Clausen, Native Mass Spectrometry Can Effectively Predict PROTAC Efficacy. *ACS Cent Sci* (2020) 6: 1223-30 DOI: 10.1021/acscentsci.0c00049.
29. X. Liu, X. Zhang, D. Lv, Y. Yuan, G. Zheng, D. Zhou, Assays and technologies for developing proteolysis targeting chimera degraders. *Future Med Chem* (2020) 12: 1155-79 DOI: 10.4155/fmc-2020-0073.
30. S.L. Lim, A. Damnernasawad, P. Shyamsunder, W.J. Chng, B.C. Han, L. Xu, J. Pan, D.P. Pravin, S. Alkan, J.W. Tyner, H.P. Koeffler, Proteolysis targeting chimeric molecules as therapy for multiple myeloma: efficacy, biomarker and drug combinations. *Haematologica* (2019) 104: 1209-20 DOI: 10.3324/haematol.2018.201483.
31. X. Li, Y. Song, Proteolysis-targeting chimera (PROTAC) for targeted protein degradation and cancer therapy. *J Hematol Oncol* (2020) 13: 50 DOI: 10.1186/s13045-020-00885-3.
32. X. Liao, X. Qian, Z. Zhang, Y. Tao, Z. Li, Q. Zhang, H. Liang, X. Li, Y. Xie, R. Zhuo, Y. Chen, Y. Jiang, H. Cao, J. Niu, C. Xue, J. Ni, J. Pan, D. Cui, ARV-825 Demonstrates Antitumor Activity in Gastric Cancer via MYC-Targets and G2M-Checkpoint Signaling Pathways. *Front Oncol* (2021) 11: 753119 DOI: 10.3389/fonc.2021.753119.
33. S. Wu, Y. Jiang, Y. Hong, X. Chu, Z. Zhang, Y. Tao, Z. Fan, Z. Bai, X. Li, Y. Chen, Z. Li, X. Ding, H. Lv, X. Du, S.L. Lim, Y. Zhang, S. Huang, J. Lu, J. Pan, S. Hu, BRD4 PROTAC degrader ARV-825 inhibits T-cell acute lymphoblastic leukemia by targeting 'Undruggable' Myc-pathway genes. *Cancer Cell Int* (2021) 21: 230 DOI: 10.1186/s12935-021-01908-w.
34. N. Kwiatkowski, T. Zhang, P.B. Rahl, B.J. Abraham, J. Reddy, S.B. Ficarro, A. Dastur, A. Amzallag, S. Ramaswamy, B. Tesar, C.E. Jenkins, N.M. Hannett, D. McMillin, T. Sanda, T. Sim, N.D. Kim, T. Look, C.S. Mitsiades, A.P. Weng, J.R. Brown, C.H. Benes, J.A. Marto, R.A. Young, N.S. Gray, Targeting transcription regulation in cancer with a covalent CDK7 inhibitor. *Nature* (2014) 511: 616-20 DOI: 10.1038/nature13393.
35. Y. Peng, S. Dong, Y. Song, D. Hou, L. Wang, B. Li, H. Wang, Key sunitinib-related biomarkers for renal cell carcinoma. *Cancer Med* (2021) 10: 6917-30 DOI: 10.1002/cam4.4206.
36. C. Dardis, D. Donner, N. Sanai, J. Xiu, S. Mittal, S.K. Michelhaugh, M. Pandey, S. Kesari, A.B. Heimberger, Z. Gatalica, M.W. Korn, A.L. Sumrall, S. Phuphanich, Gliosarcoma vs. glioblastoma: a retrospective case series using molecular profiling. *BMC Neurol* (2021) 21: 231 DOI: 10.1186/s12883-021-02233-5.
37. Y. Zhao, Z. Wang, Q. Wang, L. Sun, M. Li, C. Ren, H. Xue, Z. Li, K. Zhang, D. Hao, N. Yang, Z. Song, T. Ma, Y. Lu, Overexpression of FES might inhibit cell proliferation, migration, and invasion of osteosarcoma cells. *Cancer Cell Int* (2020) 20: 102 DOI: 10.1186/s12935-020-01181-3.
38. J.A.I. Thoms, P. Truong, S. Subramanian, K. Knezevic, G. Harvey, Y. Huang, J.A. Seneviratne, D.R. Carter, S. Joshi, J. Skhinas, D. Chacon, A. Shah, I. de Jong, D. Beck, B. Göttgens, J. Larsson, J.W.H. Wong, F. Zanini, J.E. Pimanda, Disruption of a GATA2-TAL1-ERG regulatory circuit promotes erythroid

Tables

Table 1

shRNAs used to knockdown LYL1

Name	Sequence
Homo-LYL1-sh1	CCGGAGAAGGCAGAGATGGTGTGTGCTCGAGCACACACCATCTCTGCCTTCTTTTTTTGAATT
Homo-LYL1-sh2	CCGGCACTTTGGCCCTGCACTACCACTCGAGTGGTAGTGCAGGGCCAAAGTGTTTTTTGAATT
Homo-LYL1-sh3	CCGGCTTCCTCAACAGTGTCTACATCTCGAGATGTAGACACTGTTGAGGAAGTTTTTTGAATT

Table 2

Primers used for qRT-PCR analyses

Name	Sequence (5'→3')
LYL1 Forward	ACAGTGTCTACATTGGGCCAG
LYL1 Reverse	GGCTGCTAGGGAAGATGCT
GAPDH Forward	ACAACTTTGGTATCGTGGAAGG
GAPDH Reverse	GCCATCACGCCACAGTTTC

Figures

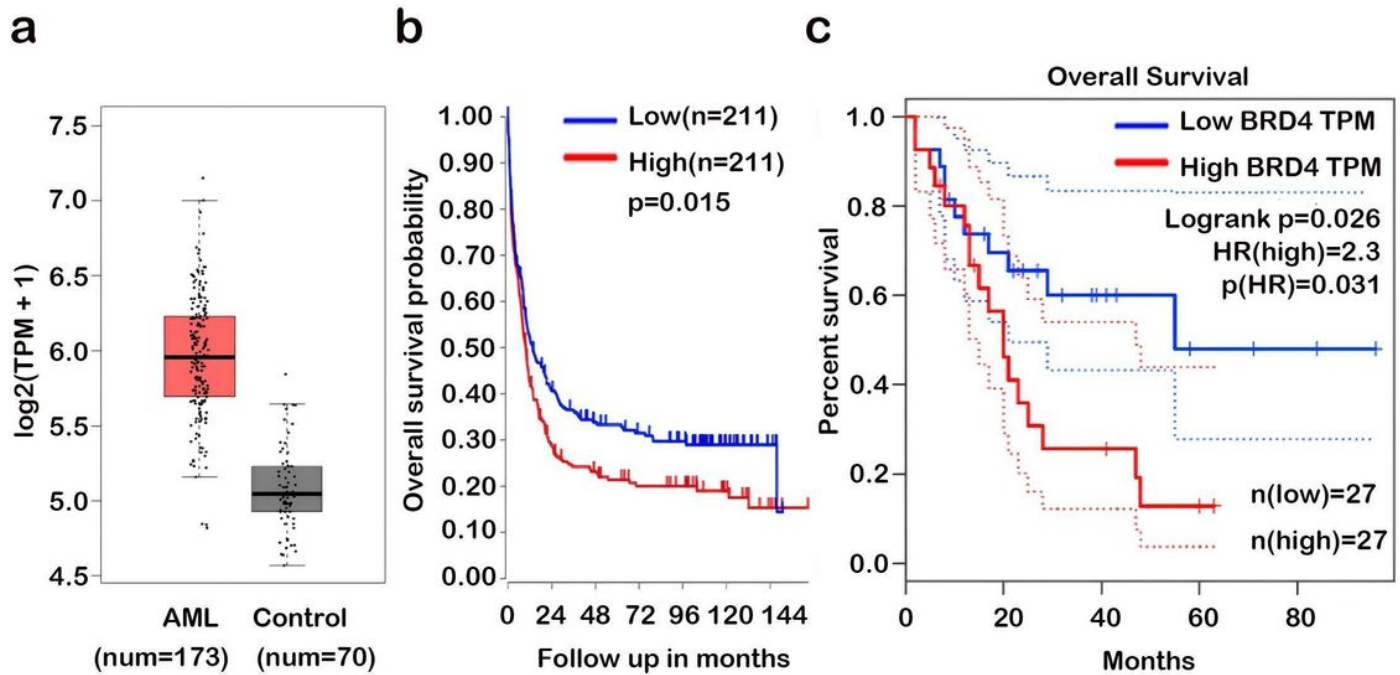


Figure 1

BRD4 is a potential good target for AML. **a** Expression of BRD4 in AML patients and normal controls according to the GEPIA database (<http://gepia.cancer-pku.cn/index.html>). **b** The expected overall survival rate of high BRD4 expression in AML patients is lower than that of low expression patients according to the R2 database (<https://hgserver1.amc.nl/cgi-bin/r2/main.cgi>). **c** The expected overall survival rate of high BRD4 expression in AML patients is lower than that of low expression patients according to the GEPIA database (<http://gepia.cancer-pku.cn/index.html>).

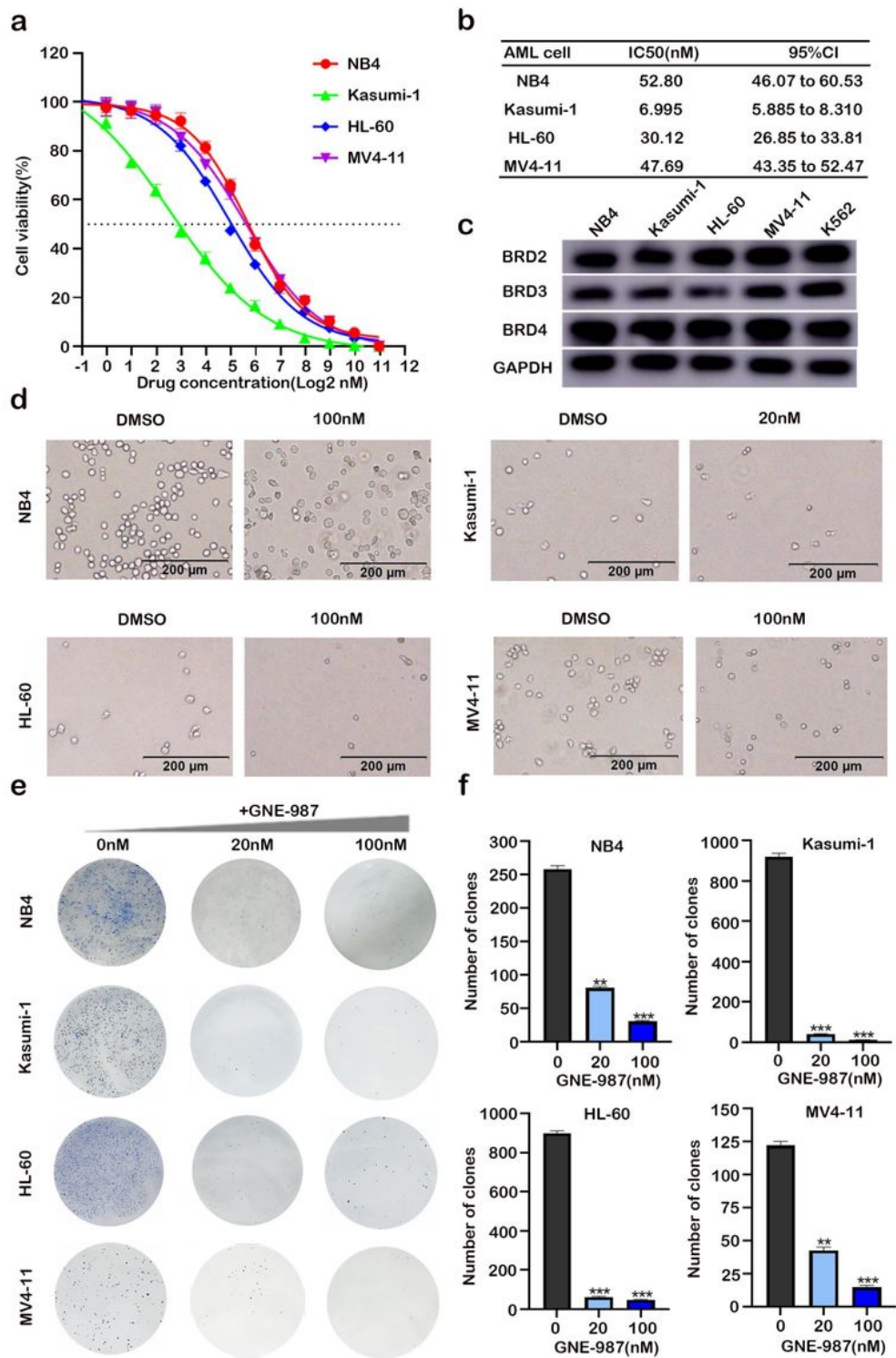


Figure 2

GNE-987 can cause the death of AML cell lines and inhibit their growth. **a** Cell viability curve after adding different concentration gradients of GNE-987 to NB4, Kasumi-1, HL-60 and MV4-11 cell lines. **b** IC50 values of GNE-987 with different concentration gradients added to AML cells. **c** The basal BET protein level analysis in myeloid cell lines NB4, Kasumi-1, HL-60, MV4-11 and K562. **d** Fluorescence microscope photos of AML cell lines NB4, Kasumi-1, HL-60, and MV4-11 24 hours after adding GNE-987. **e** The

number of AML cell clones added with different concentrations of GNE-987. **f** Statistical histogram of the number of AML cell clones added with different concentrations of GNE-987.

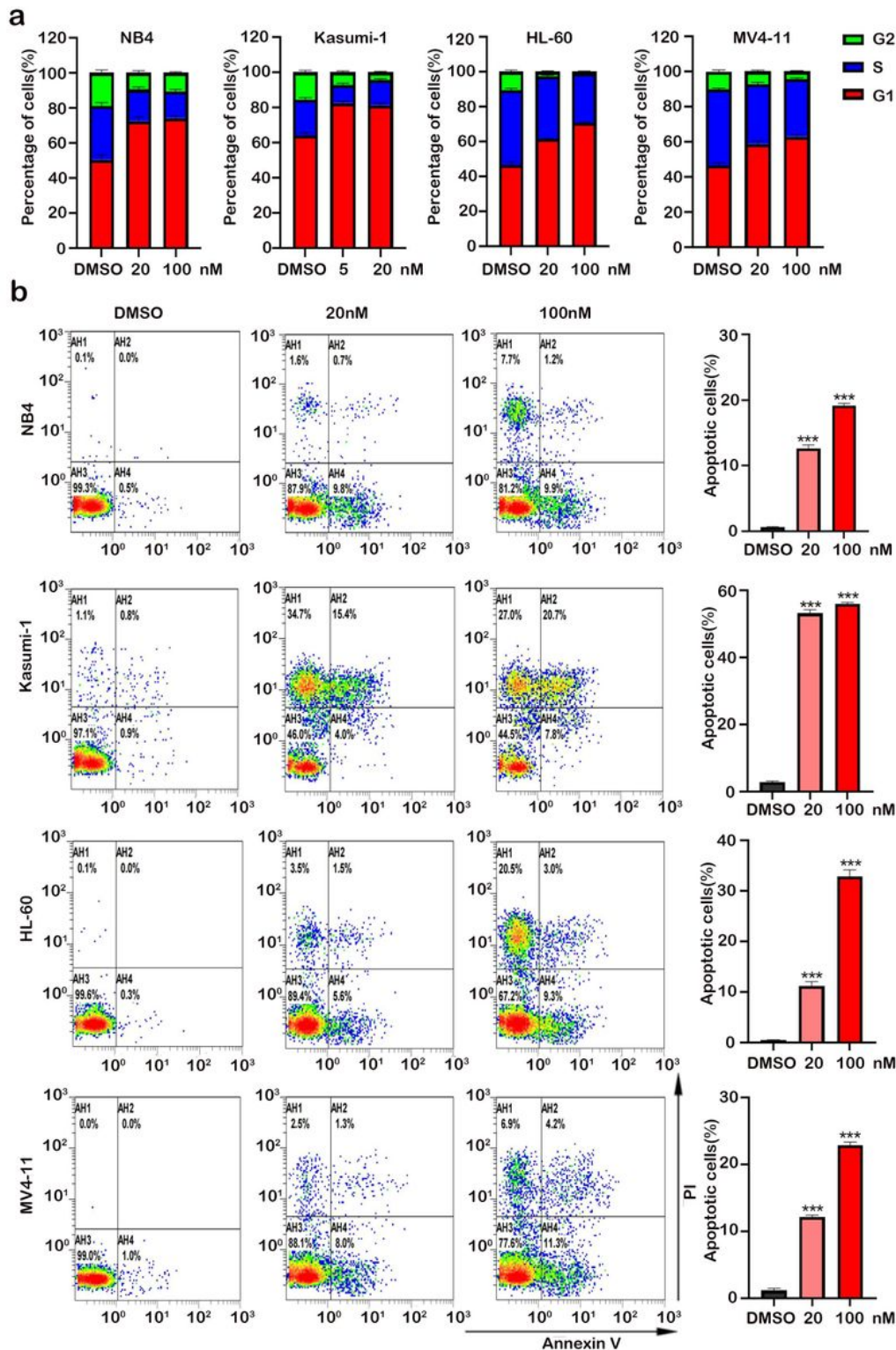


Figure 3

GNE-987 blocked cell cycle and promoted apoptosis of AML cell lines. **a** PI-labeled cell cycle of NB4, Kasumi-1, HL-60 and MV4-11 cells were analyzed after treatment with DMSO or different concentrations

of GNE-987 for 24 h. AML cells were distributed in G1/S phase and the cell population in G1 phase increased dramatically after treatment with GNE-987. **b** Annexin V and PI-labeled cell apoptosis of AML cells analyzed by flow cytometry after DMSO or different concentrations of GNE-987 treatment for 24 h. The apoptotic rates of AML cells were significantly increased after GNE-987 treatment.

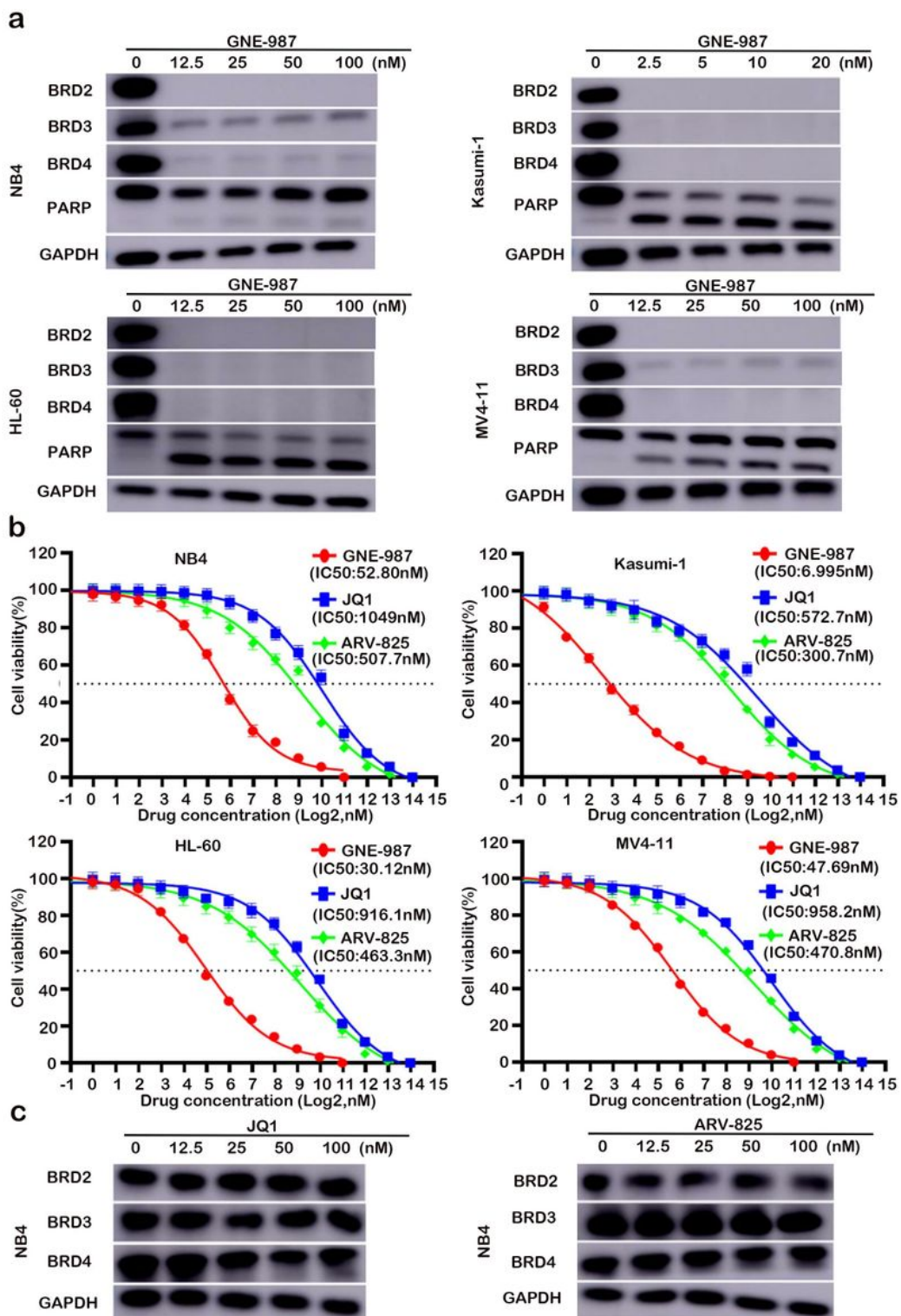


Figure 4

GENE-987 inhibits the expression of BET protein and increases the expression of PARP protein. **a** Western blotting analysis showed that GNE-987 induced BET proteins degradation, and PARP increase in NB4, Kasumi-1, HL-60 and MV4-11 cell lines. **b** Drug sensitivity assay of NB4, Kasumi-1, HL-60 and MV4-11 cell lines after treatment with gradient concentrations of GNE-987, JQ1 and ARV-825 for 24 h. **c** After adding JQ1 and ARV-825 at the highest concentration of 100 nM, the degradation efficiency of BET protein is much lower than that of GNE-987.

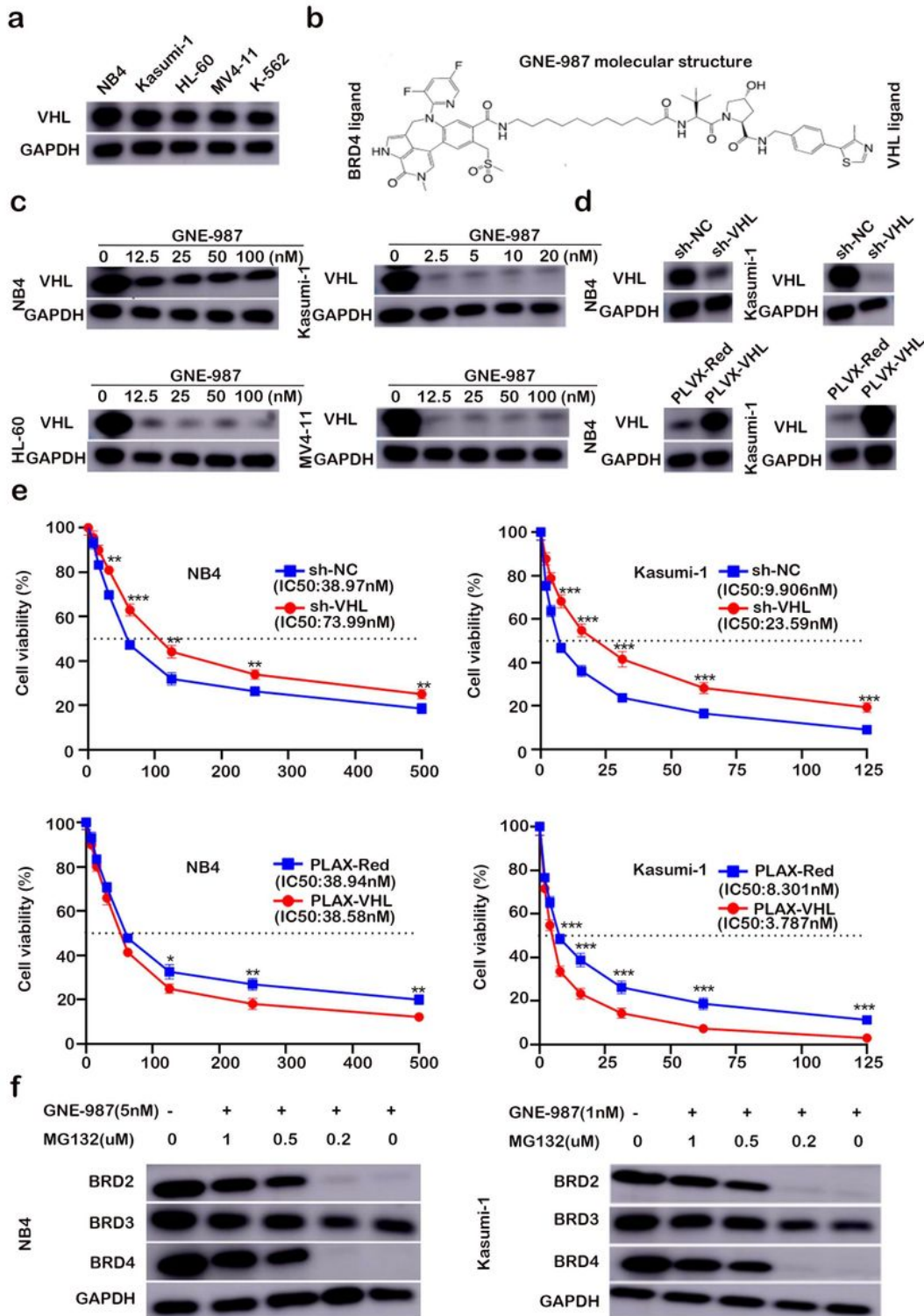


Figure 5

VHL was a powerful helper for GNE-987 in AML cells; BRDs protein degradation is proteasome-dependent. **a** Western blot analysis of VHL protein expression in AML cell lines. **b** The molecular structure of GNE-987 contains BRD4 ligand and VHL ligand. **c** Western blot analysis showed that VHL degradation increased after adding GNE-987 with different concentration gradients. **d** Knockdown / Overexpressing of VHL expression by sh-VHL lentivirus / pLX304-VHL-V5 at 5 days in NB4 and Kasumi-1 cells. **e** Down-regulated VHL increased the half-inhibitory concentration of GNE-987 in NB4 and Kasumi-1 cells, while over-expression of VHL decreased the half-inhibitory concentration of GNE-987 in these cells. **f** NB4 and Kasumi-1 cells were treated with GNE-987 and different concentration of MG132. After treatment with 24 h, BRD2, BRD3 and BRD4 protein levels were investigated by Western blotting analysis.

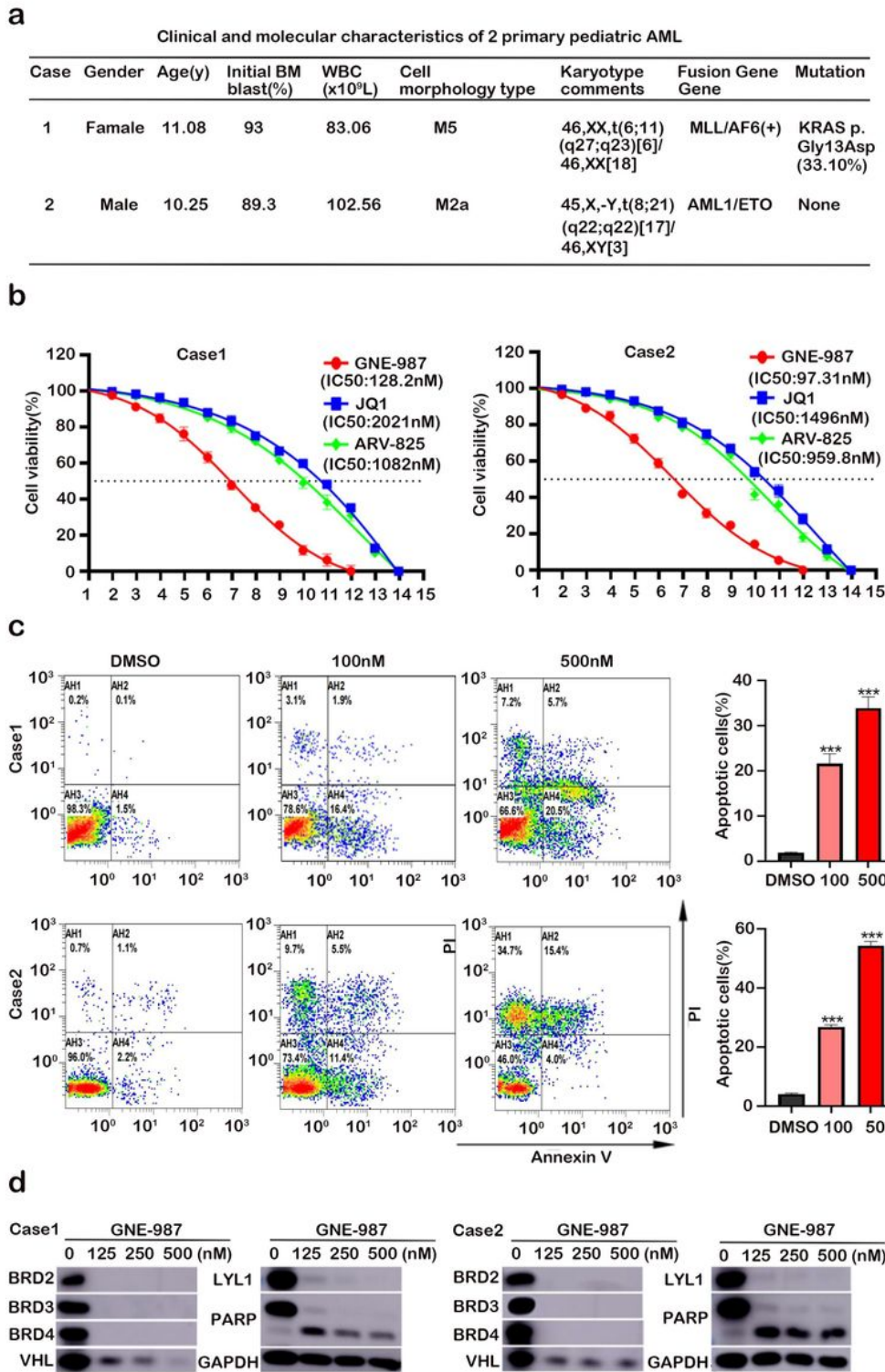


Figure 6

GNE-987 shows cytotoxicity in primary AML cells. **a** Clinical and molecular characteristics of 2 primary pediatric AML. **b** The drug sensitivity of 2 cases of primary cells treated with gradient concentrations of GNE-987, JQ1 and ARV-825 for 24 hours was determined. **c** After 24 hours of treatment with DMSO or different concentrations of GNE-987, the primary cells were analyzed for annexin V and PI-labeled apoptosis by flow cytometry. The apoptotic rate of primary cells increased significantly after GNE-987

treatment. **d** Western blotting analysis showed that GNE-987 induced degradation of BET protein, and VHL and LYL1 proteins were also down-regulated, and PARP in these primary AML cells increased.

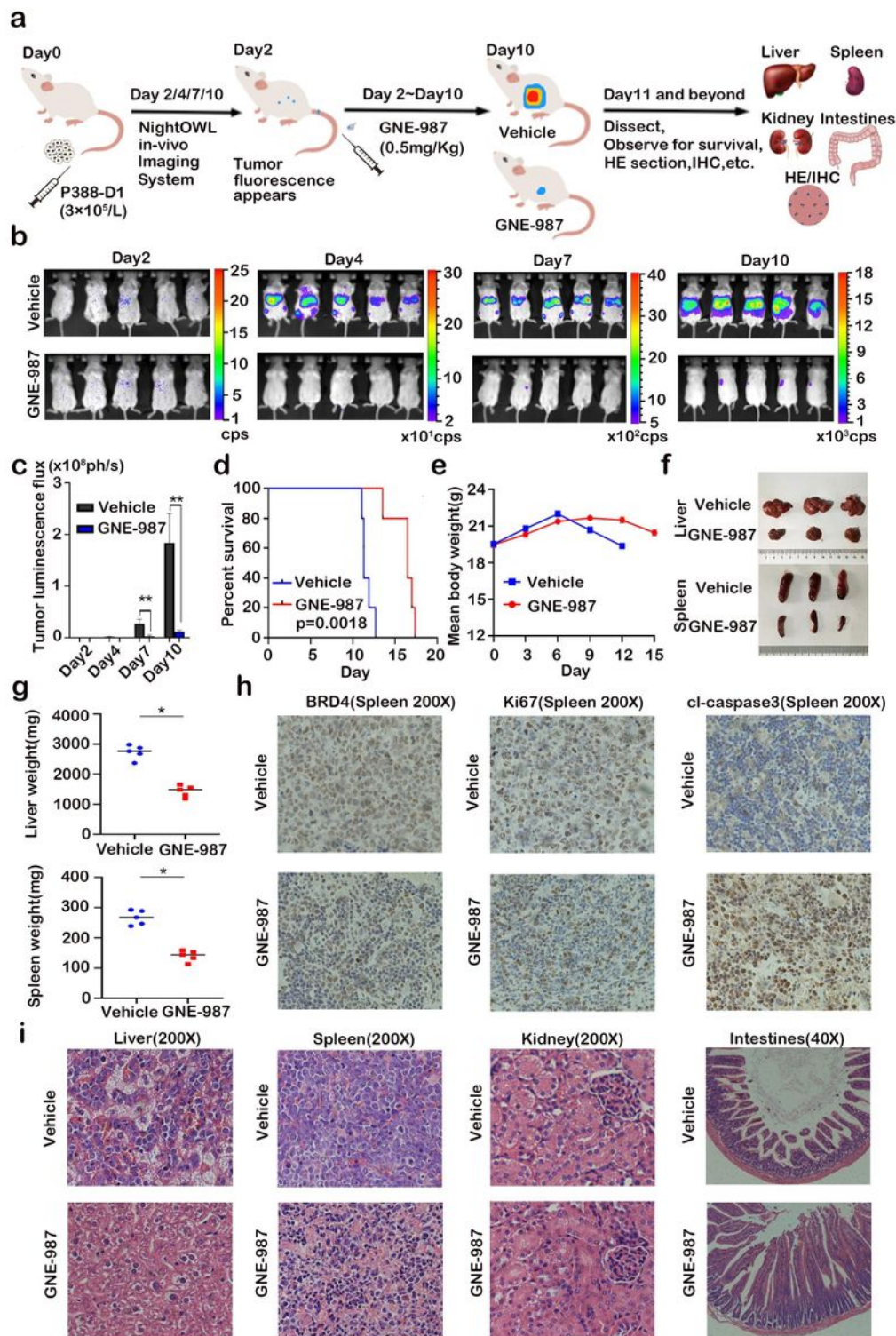


Figure 7

In vivo studies confirm that GNE-987 has a powerful anti-tumor effect. **a** Schematic diagram of the in vivo experiment. **b** On days 2, 4, 7, and 10, we use the NightOWL in vivo imaging system to image each group

of mice. **c** Comparison of the fluorescence statistics of the two groups of mice shows that GNE-987 can significantly reduce the liver and spleen infiltration in mice. **d** GNE-987 can extend the survival time of mice. **e** Comparing the body weight of the two groups of mice, there is no statistical difference. **f** Photographs of liver and spleen of two groups of mice. **g** Liver and spleen weight from GNE-987- or vehicle-treated mice. **h** IHC staining of BRD4, Ki67 and cleaved-caspase 3 in AML xenograft models from GNE-987 or vehicle-treated mice. **i** HE stained sections of liver, spleen, kidney and intestine from GNE-987 or vehicle-treated mice.

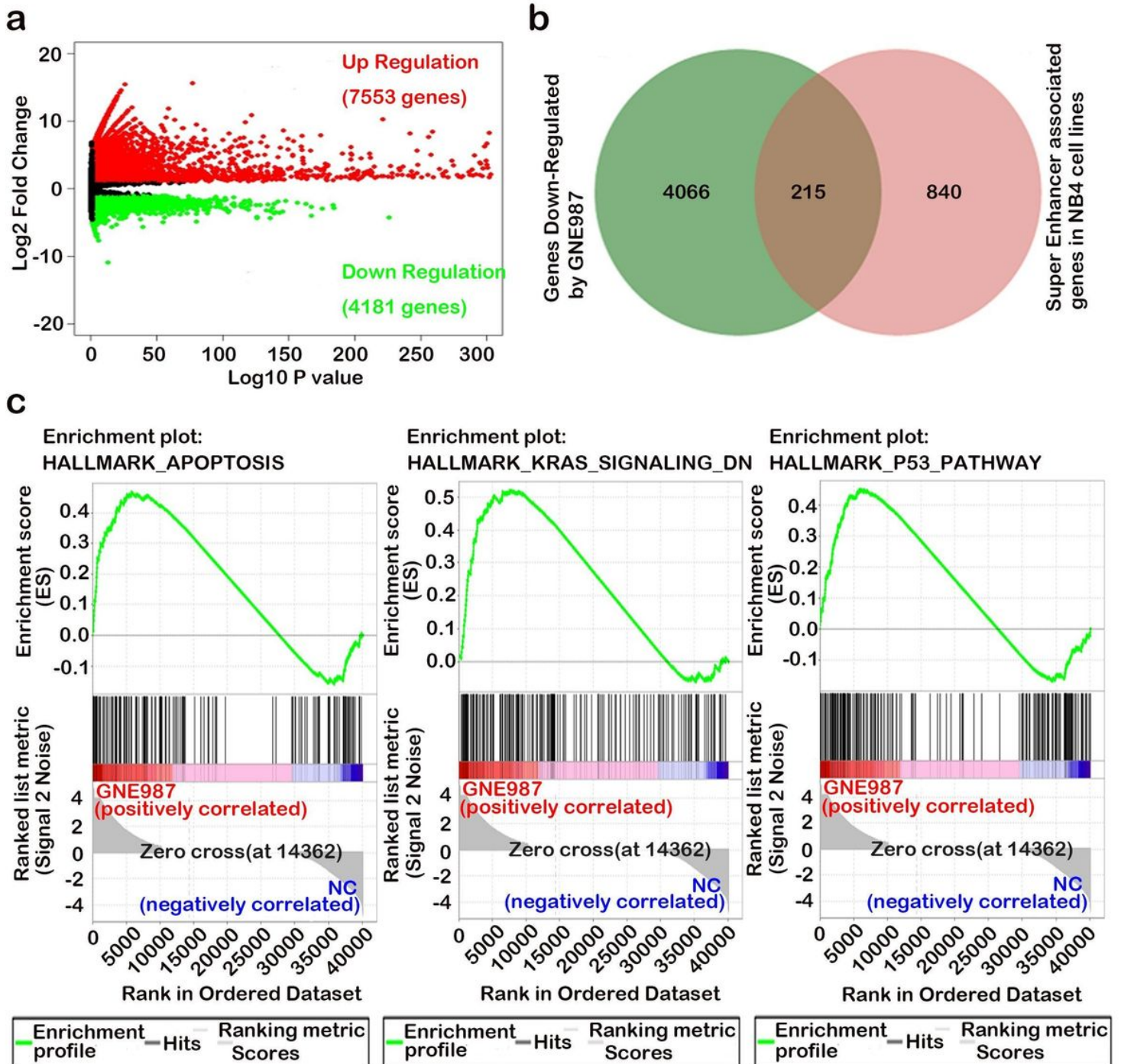


Figure 8

After AML cells are treated with GNE987, the expression of many super-enhancer-related genes is down-regulated. **a** Compared with the control group, in GNE987-treated NB4 cells, the expression of a total of 11834 genes was affected (Up-regulation of 7553 genes and down-regulation of 4281 genes). **b** Venn diagram of genes related to super enhancer and sensitive to GNE987 in NB4 cells. **c** The GSEA diagrams show that the differently expressed genes in GNE987-treated NB4 cells were enriched in the apoptosis, KRAS and P53 signaling pathways.

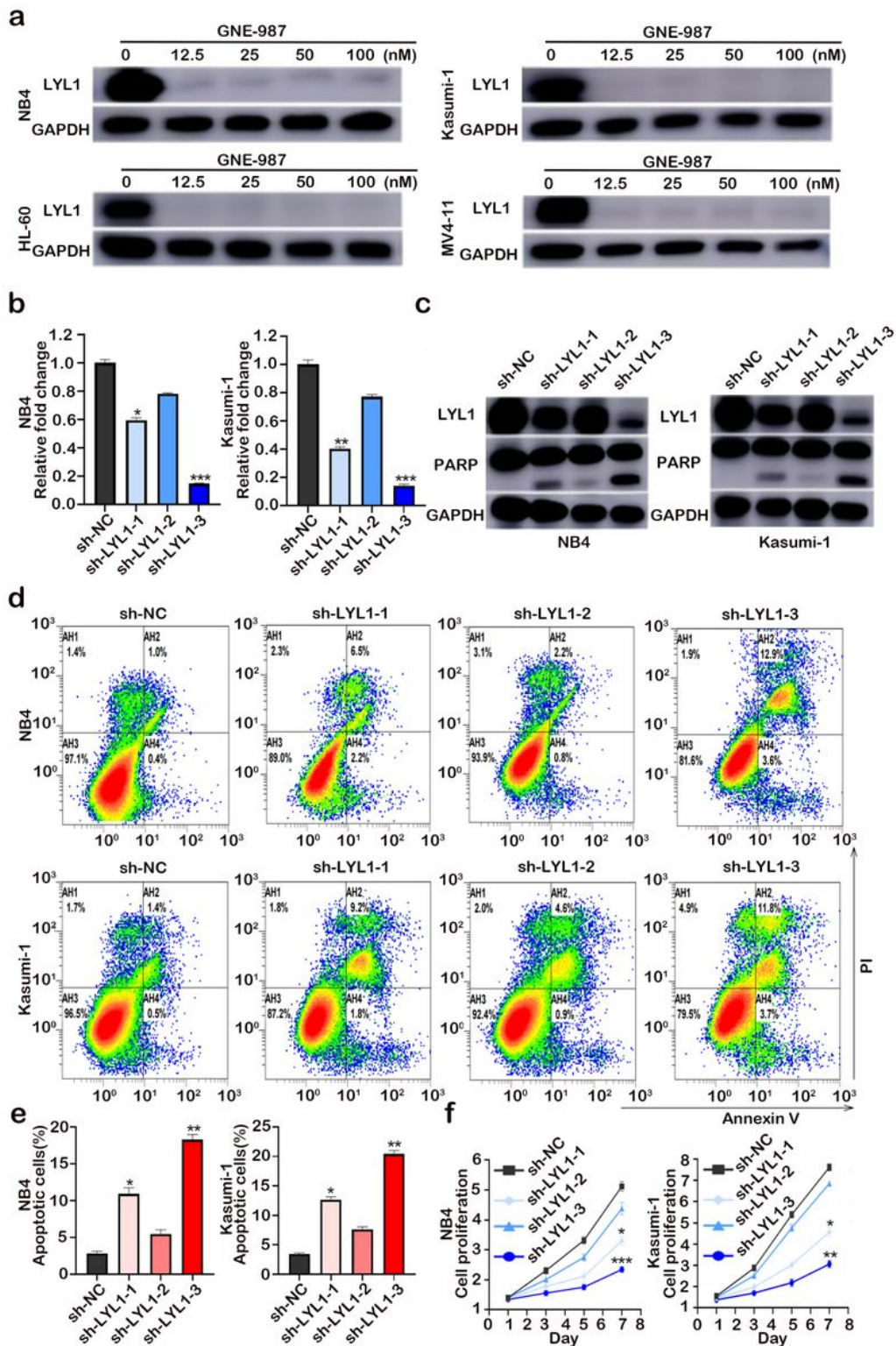


Figure 9

LYL1 is necessary for AML cell growth and survival. **a** Western blot analysis showed that after adding different concentration gradients of GNE-987 to the AML cell lines, the down-regulation of LYL1 increased. **b** Detection of LYL1 knockdown efficiency in NB4 cell line and Kasumi-1 cell line by qPCR. **c** Detection of LYL1 knockdown efficiency in NB4 cell line and Kasumi-1 cell line by western blotting. **d** Flow cytometry showed that knockdown LYL1 increased the apoptosis rate of NB4 cells and Kasumi-1 cells. **e** Statistical histogram of apoptosis rate of different sh-LYL1 sequences. **f** Knockdown of LYL1 can inhibit the proliferation rate of NB4 cells and Kasumi-1 cells.

Supplementary Files

This is a list of supplementary files associated with this preprint. Click to download.

- [Additionalfile1.psd](#)
- [Additionalfile2.psd](#)
- [Additionalfile3.psd](#)
- [Additionalfile4.psd](#)
- [Additionalfile5.psd](#)
- [Additionalfile6.psd](#)
- [Additionalfile7.psd](#)
- [Additionalfile8.psd](#)
- [Additionalfile9.psd](#)